Frontiers of Optoelectronics (2023) 16:13
https://doi.org/10.1007/s12200-023-00068-1

Frontiers of Optoelectronics

RESEARCH ARTICLE

# Two types of ultrafast mode-locking operations from an Er-doped fiber laser based on germanene nanosheets

Baohao Xu[1] · Zhiyuan Jin[1] · Lie Shi[1] · Huanian Zhang[2] · Qi Liu[3] · Peng Qin[3] · Kai Jiang[1] · Jing Wang[1] · Wenjing Tang[1] · Wei Xia[1]

Received: 22 February 2023 / Accepted: 17 April 2023


**Abstract**
As a member of Xenes family, germanene has excellent nonlinear saturable absorption characteristics. In this work, we prepared germanene nanosheets by liquid phase exfoliation and measured their saturation intensity as 0.6 GW/cm$^2$ with a modulation depth of 8%. Then, conventional solitons with a pulse width of 946 fs and high-energy noise-like pulses with a pulse width of 784 fs were obtained by using germanene nanosheet as a saturable absorber for a mode-locked Erbium-doped fiber laser. The characteristics of the two types of pulses were investigated experimentally. The results reveal that germanene has great potential for modulation devices in ultrafast lasers and can be used as a material for creation of excellent nonlinear optical devices to explore richer applications in ultrafast photonics.

**Keywords** Fiber laser · Germanene · Mode-locked · Noise-like pluses

## 1 Introduction

Ultrafast mode-locked fiber lasers with flexible structures have been widely used in various applications due to their high peak power, ultrashort pulse duration, and high stability [1–4]. Among the two common mode-locking techniques, passive mode-locking is superior to active mode-locking due to its easier self-starting, simpler structure, and better environmental stability [5]. In passively mode-locked lasers, saturable absorbers (SAs) are the key devices and can be classified into two types: real SAs and artificial SAs [6, 7]. Although artificial SAs (for example, nonlinear polarization rotation) can enable ultra-fast lasers and high-energy pulses, their high environmental sensitivity and poor stability limit their application. While real SAs with excellent nonlinear optical properties do not have these shortcomings and are being widely investigated by researchers.

In recent years, the discovery of various low-dimensional materials has significantly boosted the development of SAs, which are widely used in mode-locked fiber lasers. From the earliest graphene [8–10], to the later carbon nanotubes (CNTs) [11], transition metal dichalcogenides (TMDs) [12–17], topological insulators (TIs) [18–21], MXenes [22, 23], Xenes [24–26] and other two-dimensional (2D) materials [27, 28], all have been verified to have ultrafast saturable absorption properties. Among them, single-element Xenes, where X denotes possible elements from group IIIA to VIA, and "ene" has Latin origins indicating nanosheets, have been proven to be different from other 2D materials due to their tunable bandgap, ultra-high surface-to-volume ratio, and high carrier mobility [29]. In particular, germanene, which has been studied recently, is proven to have excellent nonlinear optical properties and has aroused widespread research interest in fields of nonlinear optics and ultrafast mode-locked lasers [30, 31]. It has superfast optical response and broadband optical absorption characteristics. In addition, the environmental stability of germanene is good [32]. However, up to now, the research on germanene is still relatively scarce, and its nonlinear optical characteristics in ultrafast optics have not been fully explored.

✉ Wenjing Tang
sps_tangwj@ujn.edu.cn

✉ Wei Xia
sps_xiaw@ujn.edu.cn

[1] School of Physics and Technology, University of Jinan, Jinan 250022, China

[2] School of Physics and Optoelectronic Engineering, Shandong University of Technology, Zibo 255049, China

[3] Shandong Huaguang Optoelectronics Co., Ltd., Jinan 250101, China

Published online: 07 June 2023

Based on low-dimensional material SA, passively mode-locked fiber lasers can generate multiple types of solitons. Therefore, passively mode-locked fiber laser is also an ideal device for studying multi-soliton dynamics [33]. By controlling the operating parameters of the laser, such as pump power, polarization state, and cavity length, a variety of soliton states can be obtained, such as soliton rain [34, 35], bound states [36, 37], higher-order harmonics [31], and noise-like pulse states. In particular, compared with the low pulse energy of conventional soliton mode-locking (CS-ML), noise-like mode-locking (NL-ML) can produce larger pulse energy [38]. The high pulse energy of mode-locked pulse in fiber lasers has always been one of the excellent characteristics sought by researchers and NL-ML fiber lasers have great potential for various applications. Usually, most of studies on multi-solitons, especially noise-like pulse (NLP), are realized by using nonlinear polarization rotation or nonlinear amplification ring mirrors, which are artificial SAs. In recent years, investigations on obtaining NL-ML using SAs based on low-dimensional materials have also been gradually reported. For instance, Guo et al. achieved typical NL-ML operation based on $WS_2$ in an erbium-doped fiber laser (EDFL), with a spectral bandwidth of 0.48 nm and laser output power of 10.2 mW, corresponding to a single pulse energy of 4.74 nJ [39]. Dong et al. obtained CS-ML with a pulse width of 439 fs and NL-ML operation with a pulse width of 1.75 ps based on single-wall CNTs at 1550 nm [40]. Zhao et al. used PbS quantum-dots as the SA in an EDFL to obtain NL-ML operation with a pulse duration of 1.6 ps and a pulse energy of 9.68 nJ [41]. However, investigations of the NL-ML operation based on real SAs are still insufficient. Therefore, it is very important to explore novel 2D SAs for mode-locking fiber lasers and investigate corresponding mechanisms.

In this paper, we have successfully prepared the germanene-PVA thin film and investigated its nonlinear optical characteristics. Then, the germanene-PVA SA was applied in an EDFL. CS-ML operation with a minimum pulse duration of 946 fs and a signal-to-noise ratio (SNR) of 80 dB was obtained at low pump powers, corresponding to a maximum pulse energy of 0.13 nJ. When the single pulse energy exceeded the energy range of the CS-ML pulse as the pump power increased, NL-ML operation was achieved with a pulse energy of 0.4 nJ, a SNR of 75 dB, and a coherent peak half-height width of 784 fs. This work indicates that germanene can be used as an excellent saturable absorber material for achieving high-energy mode-locked pulses.

## 2 Preparation and characterization of SA

Germanene nanosheets were prepared by the method of liquid phase exfoliation (LPE). The preparation steps are shown in Fig. 1. First, the bulk germanium powder was ground into fine particles in a grinding dish, and subsequently, the ground germanium powder was added to a container containing 100 mL ethanol. Then the mixture was ultrasonically shaken for 5 h with an ultrasonic cleaner and centrifuged at 1500 r/min for 20 min. Next, the supernatant was taken and mixed with 5 Wt.% PVA solution in a 1:1 ratio. After 4 h of ultrasonic treatment, a uniformly distributed germanene-PVA dispersion was obtained. Finally, the germanene-PVA solution was dropped onto a clean flat glass substrate and then placed in an oven at 35 °C for 4 h to obtain the germanene-PVA film. A 1 mm × 1 mm size germanene-PVA film was cut out and connected with a flange and sandwiched between two fiber end faces as SA.

To investigate the morphology and optical characteristics of germanene nanosheets, several characterization methods were carried out. First, as shown in Fig. 2a, a scanning electron microscopy (SEM, ZEISS Sigma 300) image of the ground germanene powder was obtained. Since the interlayer force of germanene is a weak van der Waals force, a distinct layered structure can be seen in the SEM image. The layered structure of the nanosheets can be seen by transmission electron microscopy (TEM, JEOLJEM 2100) and is shown in Fig. 2b. Figure 2c shows the high-resolution TEM (HRTEM, JEOLJEM 2100) images of germanene nanosheets, from which the lattice spacing of 0.33 nm could be determined. The Raman spectra (Horiba LabRAM HR Evolution) presented in Fig. 2d show that there is a typical Raman peak of germanene nanosheets at 298.6 $cm^{-1}$, which corresponds to the in-plane vibration mode ($E_{2g}$). The Atomic Force Microscope (AFM, Bruker Dimension Icon) was used to measure the thickness of germanene nanosheets, and the AFM image is given in Fig. 2e. Figure 2f illustrates the corresponding thickness curve. It was found that the thickness of the germanene nanosheet was 1.32 nm, corresponding to about 4 layers of germanene [42].

Subsequently, the nonlinear optical characteristics of germanene nanosheets were investigated by the dual-power detection method. Figure 3a shows the

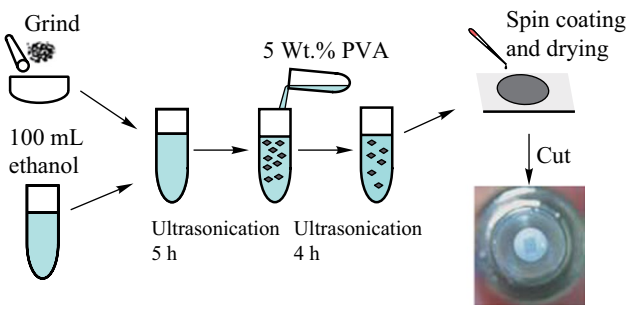


**Fig. 1** Preparation of germanene-PVA thin films

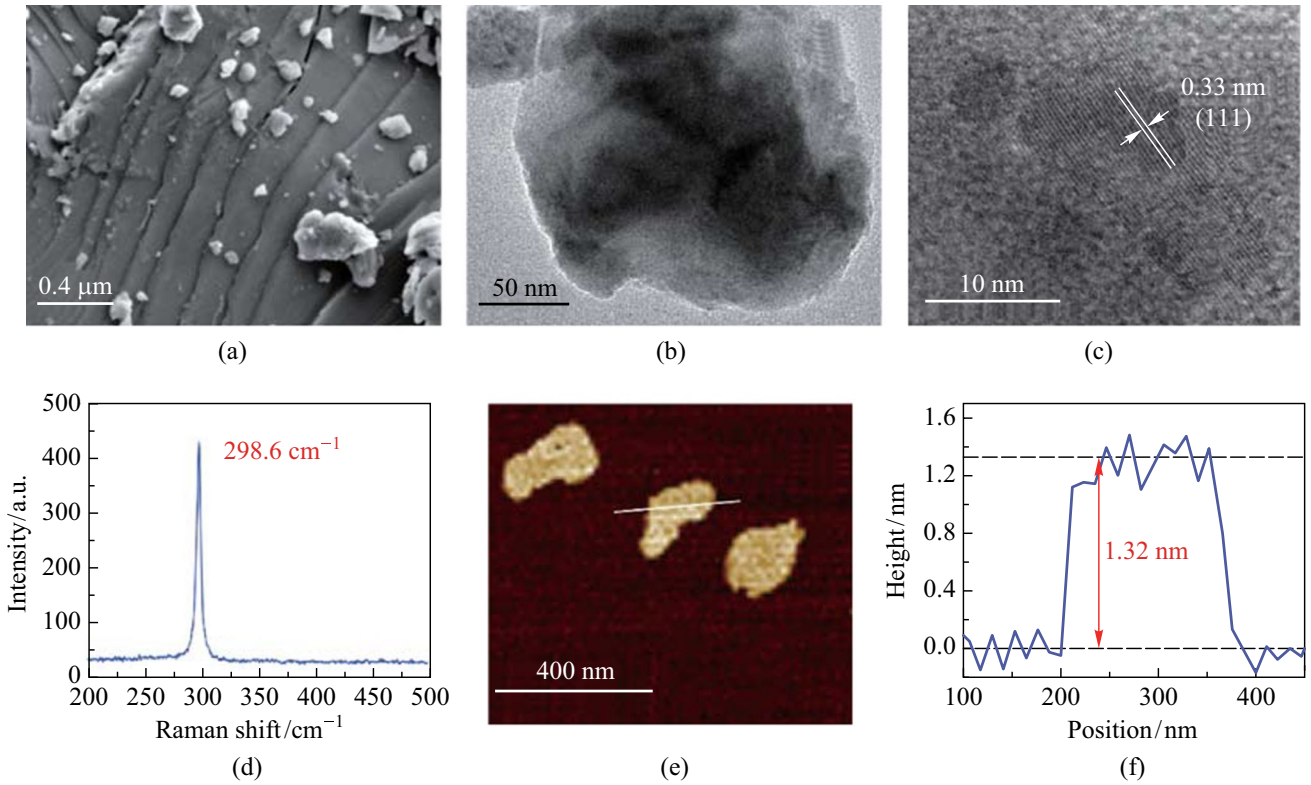


**Fig. 2** **a** SEM image of germanene, **b** TEM image, **c** HRTEM image, **d** Raman spectrum, **e** AFM image, and **f** the corresponding thicknesses curve of the germanene nanosheets

measurement setup diagram. A 1550 nm ultra-short pulse laser was used as the light source with a repetition frequency of 12.93 MHz and a pulse duration of 1.1 ps. The transmittances at different output powers are shown in Fig. 3b. The experimental data were fitted by the formula $T(I) = 1 - T_{ns} - \Delta T \cdot \exp(-I/I_{sat})$, in which $T(I)$ and $I$ are the transmission and the input intensity, respectively. The fitting value of modulation depth $\Delta T$ was 8%, corresponding to a saturation intensity $I_{sat}$ of 0.6 GW/cm$^2$. The unsaturated loss $T_{ns}$ was about 40.6%.

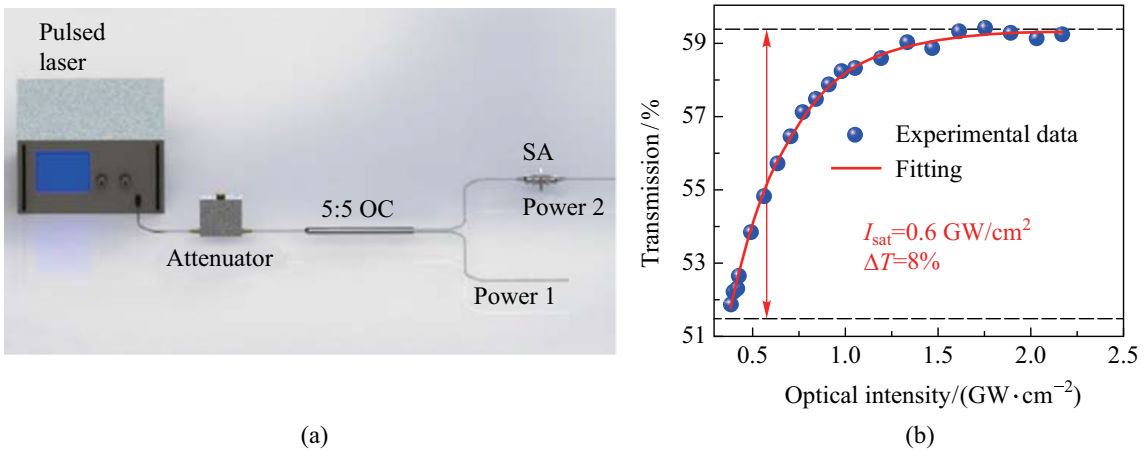


**Fig. 3** **a** Measurement setup diagram of the dual-power detection method, **b** transmission curve of the germanene-PVA SA

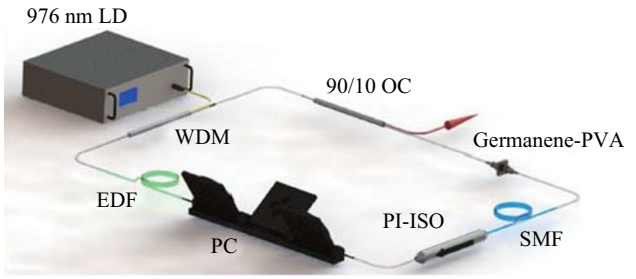


**Fig. 4** Diagram of the experimental setup of the Germanene-PVA film passively mode-locked fiber laser

## 3 Experimental setup

The experimental setup of the Germanene-PVA film passively mode-locked fiber laser is schematically illustrated in Fig. 4. A 976 nm laser diode (LD) was adopted as the pump light source with a maximum output power of 600 mW. The gain medium was a 0.3 m long erbium-doped fiber (EDF), whose group velocity dispersion (GVD) was 22.95 $ps^2$/km. The intracavity polarization state was regulated by the polarization controller (PC). The device before the PC was a polarization-independent isolator (PI-ISO) to ensure unidirectional light propagation in the laser resonant cavity. A 90:10 output coupler (OC) was used to output the 1550 nm lasing light. A thin film of germanene-PVA with a size of 1 mm × 1 mm was embedded directly between two fiber connectors as the SA. A 6.2 m long single-mode fiber (SMF) was added to make the laser operate in the negative dispersion region and reduce the repetition rate. The total cavity length was 6.5 m. The group dispersion coefficient of SMF was − 21.68 $ps^2$/km. The net dispersion of the cavity was − 0.128 $ps^2$. The pulse properties were measured by a 500 MHz mixed oscilloscope (Wavesurfer 3054z) combined with a high-speed photodetector (PD-03), an optical spectrum analyzer (Anritsu

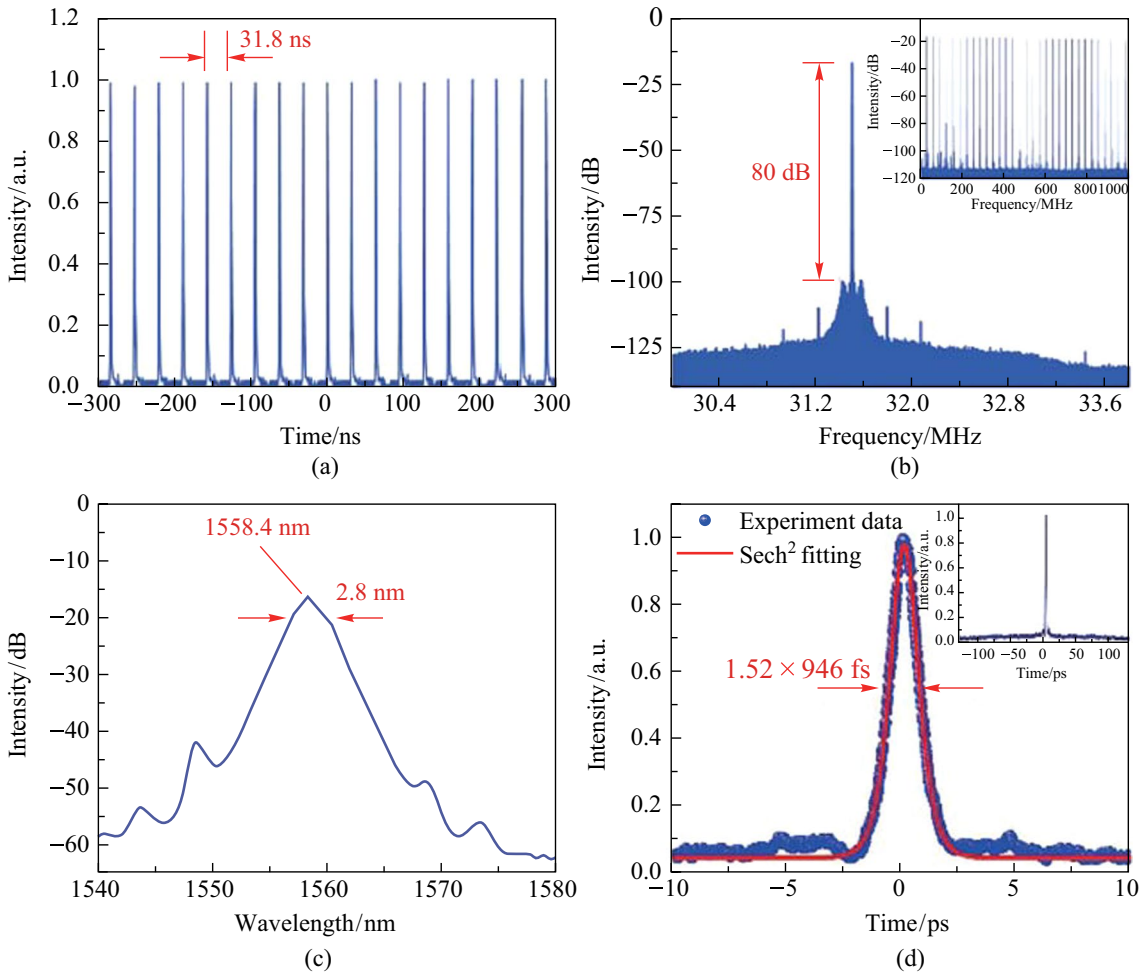


**Fig. 5** Characteristics of the CS-ML pulses at the $P_{in}$ of 251 mW: **a** the pulse trace, **b** the RF spectrum, **c** the optical spectrum, and **d** the autocorrelation trace with $sech^2$ fitting curve

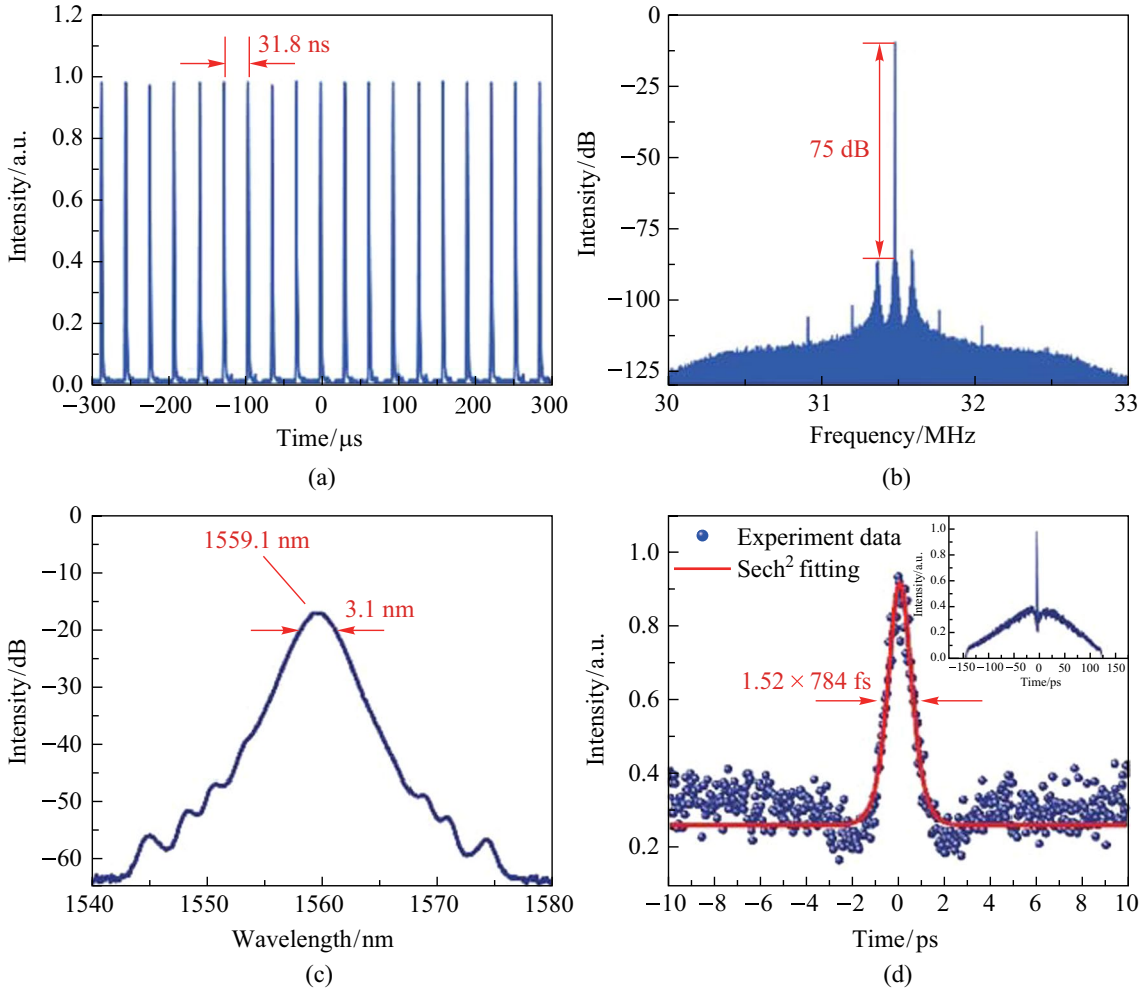


**Fig. 6** Characteristics of the NLP at the $P_{in}$ of 261.1 mW: **a** the pulse trace, **b** the RF spectrum, **c** the optical spectrum, and **d** the autocorrelation trace with sech$^2$ fitting curve

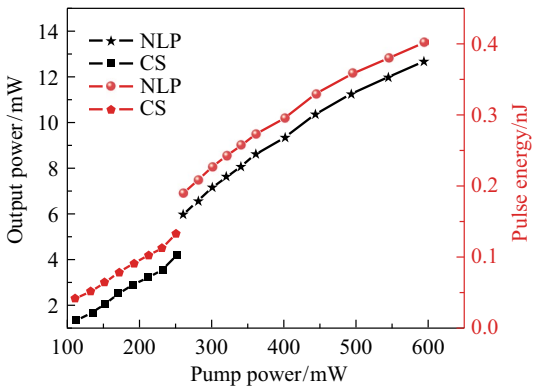


**Fig. 7** Average output powers and single pulse energies of CS-ML pulse and NL-ML pulse against $P_{in}$

MS9710C), a commercial autocorrelator (FR-103XL), an RF spectrum analyzer (Agilent N9020A), and an optical power meter.

## 4 Results and discussion

At first, to confirm that the mode-locking pulse was generated by modulation of the germanene-PVA SA, we removed the germanene nanosheet, and no matter how we adjusted the PC and pump input power ($P_{in}$) no mode-locked pulse was generated, indicating that the germanene nanosheet played a critical role in the generation of the mode-locking pulse.

Adding the SA into the cavity, stable CS-ML pulses could be obtained by carefully tuning the PC. Here, a phenomenon of $P_{in}$ hysteresis appeared. Increasing $P_{in}$ to 111.8 mW, CS-ML pulses could be first found. Then, reducing $P_{in}$ to 60.4 mW, the CS-ML could still operate stably. However, if $P_{in}$ continued to decrease until the CS-ML pulse disappeared, the pulse could only reappear when $P_{in}$ increased back to the threshold power of 111.8 mW. The trace of the mode-locked pulse sequence was recorded by oscilloscope

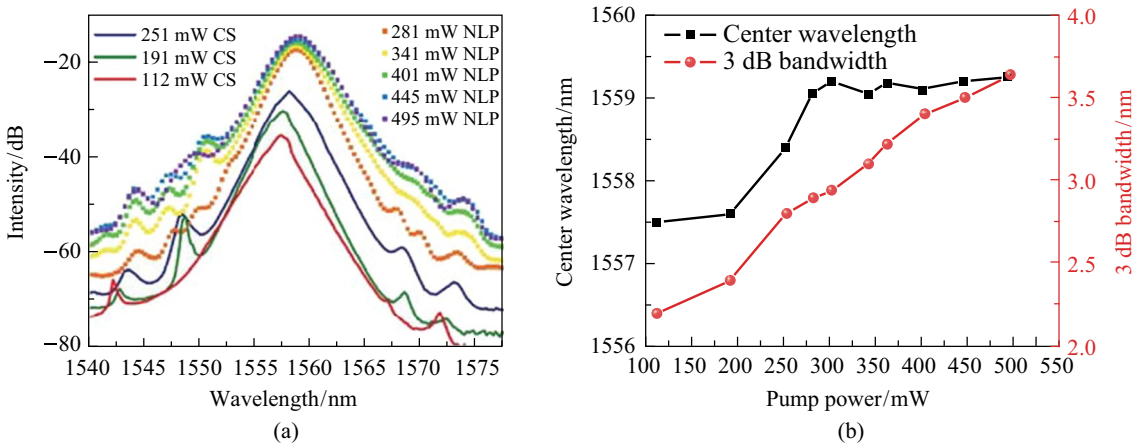


**Fig. 8** **a** Spectra at different $P_{in}$. **b** curves of spectral bandwidth and center wavelength with different $P_{in}$

at $P_{in}$ of 251 mW and illustrated in Fig. 5a. The time interval between adjacent pulses was 31.8 ns, which corresponded to a repetition frequency of 31.49 MHz. As shown in Fig. 5b, a significant SNR of 80 dB was measured. The RF spectrum in the range of 1 GHz is illustrated in the inset of Fig. 5b, showing a very consistent and stable peak, proving that the CS-ML pulse had excellent stability. Figure 5c shows the optical spectrum of the CS-ML pulse. The spectral central wavelength of the CS-ML pulse was 1558.4 nm, with a 3 dB bandwidth of 2.8 nm. The Kelly sideband caused by the dispersive wave indicated that the laser was operating in the negative dispersion region. The Kelly sidebands look a bit blurry due to the strong absorption of the resonant continuous wave background signal caused by the zero-bandgap structure of germanene SA [43]. Finally, under the $P_{in}$ of 251 mW, the pulse width of the CS-ML pulse was recorded by the autocorrelation instrument. The full width half-maximum (FWHM) of the autocorrelation trajectory was 1.46 ps, as shown in Fig. 5d. After fitting, the pulse width of 946 fs could be obtained. The corresponding time-bandwidth product (TBP) was 0.328, which was marginally larger than the theoretical value of the hyperbolic secant pulse of 0.315, indicating the existence of a minor amount of chirp.

As the $P_{in}$ continued to increase, typical NL-ML pulses could be obtained in the same laser cavity when the Pin reached 261.1 mW. This state occurred mainly caused by the interaction of multiple solitons. When the $P_{in}$ increased further, the CS-ML state became destabilized, and the soliton collapsed. The characteristics of NL-ML pulses are shown in Fig. 6. Figure 6a gives the pulse trajectory diagram at the $P_{in}$ of 261.1 mW. The NL-ML pulse operated at the basic repetition frequency, so it had the same pulse interval (31.8 ns) and repetition frequency (31.49 MHz) as the CS-ML pulse. The SNR of 75 dB was obtained and is shown in Fig. 6b, indicating that the NL-ML pulses had the same high stability as CS-ML pulses. Figure 6c demonstrates the optical spectrum of the NL-ML pulse with the spectral center wavelength at 1559.1 nm. The corresponding 3 dB bandwidth was 3.1 nm, which was larger than that of the CS-ML pulse. The autocorrelation trajectory diagram in Fig. 6d is quite different from that of the CS-ML pulse, showing a narrow coherent peak on a wide base, this is a typical characteristic of NL-ML pulse [44]. The NL-ML pulse was equivalent to a pulse envelope composed of many ultrafast sub-pulses with diverse pulse duration and peak powers. The FWHM of the coherent spike was 1.21 ps, corresponding to the pulse width of 784 fs. The TBP of 3.30 could be calculated by the pulse width and spectral bandwidth.

The output powers and single-pulse energies of both CS-ML pulses and NL-ML pulses versus the $P_{in}$ were recorded and are given in Fig. 7. Stable CS-ML pulse was achieved in the $P_{in}$ range of 111.8 to 251.6 mW, and noise-like operation was achieved in the range of 261.1 to 595.7 mW. At $P_{in}$ of 251.6 mW, the maximum output power of the CS-ML pulse was 4.23 mW, and the single pulse energy at this time was 0.13 nJ, which was consistent with the energy of conventional solitons (~0.1 nJ). For the NL-ML pulse, the maximum output power was 12.71 mW at $P_{in}$ of 595.7 mW, corresponding to a single pulse energy of 0.4 nJ, which was much higher than that of the CS-ML pulse.

To further investigate the spectral changes under different pulse mechanisms, we recorded the spectra for different $P_{in}$ values, as shown in Fig. 8. Compared with the CS-ML pulse, the spectrum of the NL-ML pulse was much smoother with a wider spectral width. However, because the single pulse energy was not large enough, there were still small sidebands in the noise-like spectra, and we believe that the spectra could have been wider as well as smoother if the $P_{in}$ had continually increased. We also measured the variation of the spectral center wavelength and 3 dB bandwidth versus the $P_{in}$. Whether in CS-ML or NL-ML operation, the 3 dB bandwidth of the laser increased with the increase of the $P_{in}$.

When the $P_{in}$ was less than 251 mW, the laser operated in the CS-ML state and the center wavelength increased with the increase of $P_{in}$; when the $P_{in}$ was greater than 261 mW, the laser entered the NL-ML state and the center wavelength was almost unchanged.

Finally, to verify the long-term stability of the fiber laser, the oscilloscope traces and optical spectra of CS-ML and NL-ML pulses were all observed for three continuous periods of 4 h, once every day for three days, at the pump powers of 251 and 597 mW. The pulse train and the central wavelength of the spectrum were always stable. No damage on the PVA film was found. It was thus experimentally demonstrated that the EDFL with germanene nanosheets as the SA can produce highly stable CS-ML pulses and large energy NL-ML pulses. It was also shown that germanene material has great potential to be used in SA devices for the generating of large energy ultrashort pulses.

## 5 Conclusion

In summary, CS-ML pulse and NL-ML pulse were successfully obtained in an EDFL using a germanene-PVA SA prepared by liquid phase stripping method. Both states were operated at a repetition frequency of 31.49 MHz. The spectral bandwidth of conventional solitons was 2.8 nm, corresponding to the pulse width of 946 fs and the single pulse energy of 0.13 nJ at a pump input power of 251 mW. In the noise-like state, the pulse width of NL-ML pulses was 784 fs, with the maximum single pulse energy of 0.4 nJ. The research confirms that the germanene material can play a great role in the study of nonlinear dynamics.

**Acknowledgements** This research was funded by the National Natural Science Foundation of China (Grant No. 62005094), the Natural Science Foundation of Shandong Province (No. ZR2021MF128), the Key research program of Shandong Province (2020JMRH0302), the Industrial Chain Program of Shandong laser Equipment Innovation and Entrepreneurship Community (JGCYL2022-5).

**Author contributions** BX and LS conceived and designed the experiments, performed the experiments and analyzed the data, drafted the manuscript; ZJ and KJ fabricated and characterized the saturable absorber; WT, JW, and WX contributed to perform the theoretical analysis; HZ, QL. and PQ provided some experimental equipment and all authors contributed to writing and editing the manuscript. All authors read and approved the final manuscript.

**Availability of data and materials** The data that support the findings of this study are available from the corresponding author, upon reasonable request.

## Declarations

**Competing interests** The authors declare that they have no competing interests.



## References

1. Keller, U.: Recent developments in compact ultrafast lasers. Nature **424**(6950), 831–838 (2003)
2. Phillips, K.C., Gandhi, H.H., Mazur, E., Sundaram, S.K.: Ultrafast laser processing of materials: a review. Adv. Opt. Photonics **7**(4), 684–712 (2015)
3. Kim, J., Song, Y.: Ultralow-noise mode-locked fiber lasers and frequency combs: principles, status, and applications. Adv. Opt. Photonics **8**(3), 465–540 (2016)
4. Banerjee, A., Budker, D., Eby, J., Kim, H., Perez, G.: Relaxion stars and their detection via atomic physics. Commun. Phys. **3**(1), 1–6 (2020)
5. Wise, F.W., Chong, A., Renninger, W.H.: High-energy femtosecond fiber lasers based on pulse propagation at normal dispersion. Laser Photonics Rev. **2**(1–2), 58–73 (2008)
6. Kurtner, F.X., Au, J.A., Keller, U.: Mode-locking with slow and fast saturable absorbers-what's the difference? IEEE J. Sel. Top. Quantum Electron. **4**(2), 159–168 (1998)
7. Xu, N., Wang, H., Zhang, H., Guo, L., Shang, X., Jiang, S., Li, D.: Palladium diselenide as a direct absorption saturable absorber for ultrafast mode-locked operations: from all anomalous dispersion to all normal dispersion. Nanophotonics **9**(14), 4295–4306 (2020)
8. Duan, L., Wang, H., Bai, J., Wang, Y., Wei, L., Chen, Z., Yu, J., Wen, J.: 844-fs mode-locked fiber laser by carboxyl-functionalized graphene oxide. Opt. Eng. **56**(11), 1 (2017)
9. Bao, Q., Zhang, H., Wang, Y., Ni, Z., Yan, Y., Shen, Z., Loh, K., Tang, D.: Atomic-layer graphene as a saturable absorber for ultrafast pulsed lasers. Adv. Funct. Mater. **19**(19), 3077–3083 (2009)
10. Hendry, E., Hale, P.J., Moger, J., Savchenko, A.K., Mikhailov, S.A.: Coherent nonlinear optical response of graphene. Phys. Rev. Lett. **105**(9), 097401 (2010)
11. Im, J.H., Choi, S.Y., Rotermund, F., Yeom, D.I.: All-fiber Er-doped dissipative soliton laser based on evanescent field interaction with carbon nanotube saturable absorber. Opt. Express **18**(21), 22141–22146 (2010)
12. Xia, H., Li, H., Lan, C., Li, C., Zhang, X., Zhang, S., Liu, Y.: Ultrafast erbium-doped fiber laser mode-locked by a

CVD-grown molybdenum disulfide ($MoS_2$) saturable absorber. Opt. Express **22**(14), 17341–17348 (2014)
13. Sathiyan, S., Velmurugan, V., Senthilnathan, K., Babu, P., Sivabalan, S.: All-normal dispersion passively mode-locked Yb-doped fiber laser using $MoS_2$-PVA saturable absorber. Laser Phys. **26**(5), 055103 (2016)
14. Shang, X., Xu, N., Zhang, H., Li, D.: Nonlinear photoresponse of high damage threshold titanium disulfide nanocrystals for Q-switched pulse generation. Opt. Laser Technol. **151**, 107988 (2022)
15. Li, L., Pang, L., Wang, R., Zhang, X., Hui, Z., Han, D., Zhao, F., Liu, W.: Ternary transition metal dichalcogenides for high power vector dissipative soliton ultrafast fiber laser. Laser Photonics Rev. **16**(2), 2100255 (2022)
16. Liu, W.J., Liu, M.L., Liu, B., Quhe, R.G., Lei, M., Fang, S.B., Teng, H., Wei, Z.Y.: Nonlinear optical properties of $MoS_2$-$WS_2$ heterostructure in fiber lasers. Opt. Express **27**(5), 6689–6699 (2019)
17. Liu, M., Wu, H., Liu, X., Wang, Y., Lei, M., Liu, W., Guo, W., Wei, Z.: Optical properties and applications of $SnS_2$ SAs with different thickness. Opto-Electron. Adv. **4**(10), 200029 (2021)
18. Sotor, J., Sobon, G., Macherzynski, W., Abramski, K.: Harmonically mode-locked Er-doped fiber laser based on a $Sb_2Te_3$ topological insulator saturable absorber. Laser Phys. Lett. **11**(5), 055102 (2014)
19. Liu, H., Zheng, X.W., Liu, M., Zhao, N., Luo, A.P., Luo, Z.C., Xu, W.C., Zhang, H., Zhao, C.J., Wen, S.C.: Femtosecond pulse generation from a topological insulator mode-locked fiber laser. Opt. Express **22**(6), 6868–6873 (2014)
20. Zhang, C., Chu, H., Pan, Z., Pan, H., Zhao, S., Li, D.: Single crystalline BiOCl nanosheets with oxygen vacancies for ultrafast mode-locking operation. Opt. Laser Technol. **159**, 108945 (2023)
21. Liu, W., Xiong, X., Liu, M., Xing, X., Chen, H., Ye, H., Han, J., Wei, Z.: $Bi_4Br_4$-based saturable absorber with robustness at high power for ultrafast photonic device. Appl. Phys. Lett. **120**(5), 053108 (2022)
22. Wang, L., Li, X., Wang, C., Luo, W., Feng, T., Zhang, Y., Zhang, H.: Few-layer Mxene $Ti_3C_2T_x$ (T=F, O, Or OH) for robust pulse generation in a compact Er-doped fiber laser. ChemNanoMat **5**(9), 1233–1238 (2019)
23. Jhon, Y.I., Koo, J., Anasori, B., Seo, M., Lee, J.H., Gogotsi, Y., Jhon, Y.M.: Metallic MXene saturable absorber for femtosecond mode-locked lasers. Adv. Mater. **29**(40), 1702496 (2017)
24. Xu, N., Ma, P., Fu, S., Shang, X., Jiang, S., Wang, S., Li, D., Zhang, H.: Tellurene-based saturable absorber to demonstrate large-energy dissipative soliton and noise-like pulse generations. Nanophotonics **9**(9), 2783–2795 (2020)
25. Song, Y., Liang, Z., Jiang, X., Chen, Y., Li, Z., Lu, L., Ge, Y., Wang, K., Zheng, J., Lu, S., Ji, J., Zhang, H.: Few-layer antimonene decorated microfiber: ultra-short pulse generation and all-optical thresholding with enhanced long term stability. 2D Materials **4**(4), 045010 (2017)
26. Lu, L., Liang, Z., Wu, L., Chen, Y., Song, Y., Dhanabalan, S., Ponraj, J., Dong, B., Xiang, Y., Xing, F., Fan, D., Zhang, H.: Few-layer bismuthene: sonochemical exfoliation, nonlinear optics and applications for ultrafast photonics with enhanced stability. Laser Photonics Rev. **12**(1), 1700221 (2018)
27. Liu, W., Liu, M., Yin, J., Chen, H., Lu, W., Fang, S., Teng, H., Lei, M., Yan, P., Wei, Z.: Tungsten diselenide for all-fiber lasers with the chemical vapor deposition method. Nanoscale **10**(17), 7971–7977 (2018)
28. Liu, W., Zhu, Y., Liu, M., Wen, B., Fang, S., Teng, H., Lei, M., Liu, L., Wei, Z.: Optical properties and applications for $MoS_2$-$Sb_2Te_2$-$MoS_2$ heterostructure materials. Photon. Res. **6**(3), 220–227 (2018)
29. Zhang, H., Sun, S., Shang, X., Guo, B., Li, X., Chen, X., Jiang, S., Zhang, H., Ågren, H., Zhang, W., Wang, G., Lu, C., Fu, S.: Ultrafast photonics applications of emerging 2D-Xenes beyond graphene. Nanophotonics **11**(7), 1261–1284 (2022)
30. Mu, H., Liu, Y., Bongu, S.R., Bao, X., Li, L., Xiao, S., Zhuang, J., Liu, C., Huang, Y., Dong, Y., Helmerson, K., Wang, J., Liu, G., Du, Y., Bao, Q.: Germanium nanosheets with dirac characteristics as a saturable absorber for ultrafast pulse generation. Adv. Mater. **33**(32), e2101042 (2021)
31. Sun, W., Jiang, K., Tang, W., Su, J., Chen, K., Liu, Q., Xia, W.: Germanene nanosheets for mode-locked pulse generation in fiber lasers. Infrared Phys. Technol. **123**, 104128 (2022)
32. Li, C., Kang, J., Xie, J., Wang, Y., Zhou, L., Hu, H., Li, X., He, J., Wang, B., Zhang, H.: Two-dimensional monoelemental germanene nanosheets: facile preparation and optoelectronic applications. J. Mater. Chem. **8**(46), 16318–16325 (2020)
33. Tang, D.Y., Zhao, L.M., Zhao, B., Liu, A.: Mechanism of multisoliton formation and soliton energy quantization in passively mode-locked fiber lasers. Phys. Rev. A **72**(4), 043816 (2005)
34. Chouli, S., Grelu, P.: Rains of solitons in a fiber laser. Opt. Express **17**(14), 11776–11781 (2009)
35. Chouli, S., Grelu, P.: Soliton rains in a fiber laser: an experimental study. Phys. Rev. A **81**(6), 063829 (2010)
36. Tang, D.Y., Man, W.S., Tam, H.Y., Drummond, P.: Observation of bound states of solitons in a passively mode-locked fiber laser. Phys. Rev. A **64**(3), 033814 (2001)
37. Hsiang, W.W., Chang, C.H., Cheng, C.P., Lai, Y.: Passive synchronization between a self-similar pulse and a bound-soliton bunch in a two-color mode-locked fiber laser. Opt. Lett. **34**(13), 1967–1969 (2009)
38. Zheng, X.W., Luo, Z.C., Liu, H., Zhao, N., Ning, Q.Y., Liu, M., Feng, X., Xing, X., Luo, A., Xu, W.: High-energy noiselike rectangular pulse in a passively mode-locked figure-eight fiber laser. Appl. Phys. Express **7**(4), 042701 (2014)
39. Guo, B., Li, S., Fan, Y., Wang, P.: Versatile soliton emission from a $WS_2$ mode-locked fiber laser. Opt. Commun. **406**, 66–71 (2018)
40. Dong, Z., Tian, J., Li, R., Cui, Y., Zhang, W., Song, Y.: Conventional soliton and noise-like pulse generated in an Er-doped fiber laser with carbon nanotube saturable absorbers. Appl. Sci. (Basel) **10**(16), 5536 (2020)
41. Zhao, W., Huang, Q., Li, K., Gao, C., Cheng, X., Yan, Y., Guo, Q., Sun, X., Mou, C.: High-energy noise-like pulses generated by an erbium-doped fiber laser incorporating a PbS quantum-dot polystyrene composite film. J. Phys. Photonics **3**(2), 024015 (2021)
42. Zhuang, J., Liu, C., Zhou, Z., Casillas, G., Feng, H., Xu, X., Wang, J., Hao, W., Wang, X., Dou, S.X., Hu, Z., Du, Y.: Dirac signature in germanene on semiconducting substrate. Adv. Sci. (Weinh.) **5**(7), 1800207 (2018)
43. Wang, Y., Fu, S., Kong, J., Komarov, A., Klimczak, M., Buczyński, R., Tang, X., Tang, M., Qin, Y., Zhao, L.: Nonlinear Fourier transform enabled eigenvalue spectrum investigation for fiber laser radiation. Photon. Res. **9**(8), 1531–1539 (2021)
44. Wang, Z., Wang, Z., Liu, Y.G., Zhao, W., Zhang, H., Wang, S., Yang, G., He, R.: Q-switched-like soliton bunches and noise-like pulses generation in a partially mode-locked fiber laser. Opt. Express **24**(13), 14709–14716 (2016)

**Baohao Xu** received the B.Eng. degree in Optoelectronic Information Science and Engineering from University of Jinan, Jinan, China, in 2020, where he is currently pursuing the M.Eng. degree with the School of Physics and Technology, University of Jinan. He joined the Laser Devices and Applications Laboratory, University of Jinan, in 2021, where he was involved in research on nonlinear optics and laser technology under the supervision of Prof. Xia. His recent research interests include nonlinear optics, laser applications, and laser technology.

**Zhiyuan Jin** received the B.Eng. degree in Computer Science and Technology from University of Jinan, Jinan, China, in 2020, where he is currently pursuing the M.Eng. degree with the School of Physics and Technology, University of Jinan. He joined the Laser Devices and Applications Laboratory, University of Jinan, in 2021, where he was involved in research on semiconductor laser devices and applications under the supervision of Prof. Xia. His recent research interests include laser applications and optical engineering.

**Lie Shi** obtained the B.Eng. degree from Shandong University of Science and Technology of China in 2020. She is currently pursuing the M.S. degree with the School of Physics and Technology, University of Jinan, Jinan, China. Her research interests include fiber lasers and nonlinearoptics.

**Huanian Zhang** received the B.Eng. degree in Electronic Science and the Ph.D. degree in Optical Engineering from Shandong University, Jinan, China, in 2010 and 2015, respectively. He joined the School of Physics and Optoelectronic Engineering, Shandong University of Technology, China, in 2019. His recent research interests include new laser technology, new optoelectronic materials and devices, ultrafast photonics.

**Qi Liu** received the B.Eng. degree in Electronic Materials and Components from Harbin University of Science and Technology, China, in 1999. He joined Shandong Huaguang Optoelectronics Co., Ltd., Jinan, China, in 2002. His recent research interests include Semiconductor laser technology.

**Peng Qin** received the B.Eng. degree in Finance from Shandong Jianzhu University, China, in 2001. He joined Shandong Huaguang Optoelectronics Co., Ltd., Jinan, China, in 2002. His recent research interests include Semiconductor laser technology.

**Kai Jiang** received the B.Eng. degree in Materials Science and Engineering and the Ph.D. degree in Materials Physics and Chemistry from Shandong University, Jinan, China, in 2007 and 2014, respectively. He joined the School of Physics and Technology, University of Jinan, China, in 2017. His recent research interests include Semiconductor laser technology, nonlinear optics, and semiconductor materials.

**Jing Wang** received the B.Eng. degree in Optoelectronic Information Science and Engineering and the Ph.D. degree in Optical Engineering from Shandong University, Jinan, China, in 2001 and 2008, respectively. She joined the School of Physics and Technology, University of Jinan, China, in 2008. Her recent research interests include nonlinear optics, lasers, and laser physics and technology.

**Wenjing Tang** received the B.Eng. degree in Electronic Science and Technology, the M.Eng. degree in Optical Engineering, and the Ph.D. degree in Optical Engineering from Shandong University, Jinan, China, in 2008, 2011, and 2018, respectively. She joined the School of Physics and Technology, University of Jinan, China, in 2018. Her recent research interests include nonlinear optics, lasers, and laser technology.

**Wei Xia** received the Ph.D. degree in Optical Engineering from Shandong University, Jinan, China. He is now a professor of University of Jinan, China. His main research interests include semiconductor laser device and application, optical engineering.